Macromol. Symp. ***185,*** *149–166 (2002)*

The Effect of Natural Rubber Crosslink Density on Real Time Birefringence, True Stress and True Strain Behavior

*D. Valladares, S. Toki, T. Z. Sen , B. Yalcin, and M. Cakmak**

Polymer Engineering Institute, University of Akron, Akron, OH 44325-0301, USA

Summary: A newly developed real time spectral birefringence technique was implemented to follow the coupled relationships between birefringence, true stress and true strain behavior of varying crosslink density natural rubber vulcanizates at room temperature. It was shown that the stress optical law is valid even at early stages of crystallization during stretching and there exists a critical birefringence beyond which the metastable "near perfect" oriented and highly distorted crystalline regions form and upon retraction this crystalline order disappears at the same critical birefringence level. These crystalline regions exhibit nematic order with significant axial registry distortions at early stages of the formation. They are suggested to form at or near the juncture points of the chemical network formed by crosslinks, and physical network by chain entanglements where the orientability of the chains is the most efficient.

Introduction

Natural Rubber is probably the most important rubber material among other elastomers, especially in the tire industry. One of the principal characteristics of this material is its ability to crystallize under deformation. The strain induced crystallization (SIC) of rubbers has been widely studied in the past, however many details of the molecular reorganization that take place during stretching are not well understood. This is primarily as a result of having to use off line "snap shot" experiments performed to reveal the details of the molecular processes that continuously change during and after stretching as these polymeric chains remain mobile at room temperature since their Tg are well bellow it.

We have developed a real-time measuring system to analyze the molecular orientation and its mechanical response during uniaxial deformation with automated spectral birefringence technique. This instrument allows simultaneous recording of force, sample width, optical retardation and strain during uniaxial deformation that allows the determination of thickness and retardation during stretching. The first suggestion of the

CCC 1022-1360/00/$ 17.50+.50/0

use of continuous visible spectrum to determine birefringence was made by Yang [1] followed by Harding[2].

In a series of papers by Pluta,[3] Burghardt[4,5,6,7] this technique steadily improved over the years.[8] In these previous studies the spectral birefringence technique was not automated and made in to the real time measurement system. In order to develop a robust and fully automated system we utilized the progresses given above and developed an extensive analysis system utilizing the principles of Spectral Birefringence technique and made it fully automated as demonstrated in publications by Serhatkulu and Cakmak.[9,10,11] This enabled us to follow the very rapid retardation (and thus birefringence measurement) changes that take place in annealing of oriented films under constraint. The system was able to track changes as little as 0.2 sec real time indefinitely [10,11].

The automated spectral birefringence system was found to be sensitive enough to follow the small changes in retardation in the natural rubber that inherently possesses low intrinsic birefringence. This data is then converted to real time birefringence through on-line measurement of thickness through laser detection system. Details of this instrumentation are discussed elsewhere.[12] We have shown that the real time determination of true stress, true strain and birefringence data allows for fundamental understanding of the molecular mechanisms – orientation, crystallization, relaxation that take place during deformation without the need to stop and examine the samples revealing more realistic behavior of the materials in their actual use. This study focuses on the effect of the crosslink density on the molecular orientation and crystallization during uniaxial deformation at room temperature.

Experimental

Materials and Equipment

SMR-L (Standard Malaysian Rubber) low impurity grade Natural Rubber was used. This provided high clarity medium that was necessary for spectral birefringence measurements. The ingredients added to the rubber in order to achieve the vulcanization process are listed in Table 1. The stretching machine shown in Figure 1 was designed to stretch both top and bottom cross head in opposing directions in order to maintain mid observation point stationary. At this mid section of the sample, the spectral birefringence is measured using the automated system.[12] This system allows the measurement of retardation at about 0.4 seconds intervals. In order to determine the birefringence, the real time thickness needs to be obtained as well. This was accomplished using a laser micrometer mounted at an oblique angle that ensures the width measurement of the sample at the same position as the retardation measurement was made. This allowed us to continuously monitor width during stretching. Transverse isotropy assumption was made in order to determine the time variation of local thickness as well as true stress and true strain. The crosslink density measurements were performed using the semi-empirical equation suggested by Mooney and Rivlin (equation 1). This was in good agreement with the results obtained by swelling techniques for natural rubber samples.[13,14]

$$M_c(G_e) = A_\varphi \rho RT/G_e \qquad \text{Eq. 1}$$

$$\sigma = \sigma_0(\lambda) + G_e(\lambda^2 - \lambda^{-1})$$

where:

σ=True stress

λ=Extension ratio

ρ=Density of the rubber

Mc=Average molecular weight between crosslinks.

R=Gas Constant

$A\phi$=Prefactor (assumed to be 1)

Ge=Modulus

The average molecular weight between crosslinks (M_c) was the measured parameter that is related to the crosslink density. In this study, the lower and higher crosslink density has a Mc=8300 gr/mol and a Mc=6680g/mol respectively.

Table 1 Formulation of the natural rubber samples

INGREDIENT	**RECIPE #1 (Parts)**	**RECIPE #2 (Parts)**
SMR-L	100	100
Antioxidant	1	1
Zinc Stearate	3	4.5
Accelerant TBBS	1	1.5
Sulfur	1	1.5

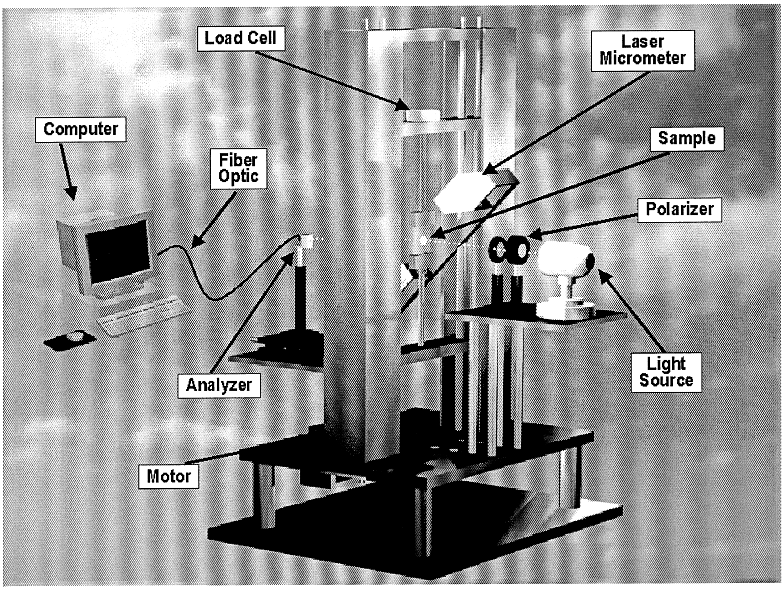

Figure 1. Spectral Birefringence – Stretching Machine.

X-Ray Measurements

In order to examine the state of crystalline order and orientation at different extension levels, the sample in the strained state was captured in a rectangular sandwich clamp and WAXS patterns were taken immediately off line using a GE XRD-6 X-ray generator equipped with a WAXS-SAXS combination camera. WAXS patterns were taken at the same central observation point where the real time birefringence and width were monitored.

Flat film WAXS patterns were obtained using exposure time of 1.5 hours. The total time between the end of the on-line experiment and the end of the X-ray measurement did not exceed 2 hours.

Results and Discussions

Mechanical Behavior

Figures 2 and 3 shows the mechanical response of the natural rubber during stretching at room temperature for two crosslink densities. The superposed curves are the data obtained on samples stretched to different levels (2X, 3X, 4X and 5X). Figure 2 and Figure 3 shows the plot of engineering stress vs. engineering strain and the behavior of the true stress with respect to the true strain respectively. Both cases display a typical behavior observed for elastomers showing a progressive increase of the stress-true stress as the strain-true strain reaches higher values. However, the shape of the curves, particularly the slope of the curves at early stages of the deformation, is distinctly different. The true stress rises slower with true strain. The engineering stress-strain curves exhibit artificially high stresses at early stages of deformation.

Two main observations for different crosslink density samples are clear. The higher crosslink density sample shows higher values of stress for a fixed value of strain and modulus increases with increasing amounts of chemical crosslinks.

Figure 4 shows the true stress behavior with time for samples stretched at 30mm/min stretching rate. The natural rubber samples were stretched to 2x, 3x, 4x, and 5x for both crosslink densities followed by a relaxation process where the samples were kept at the final strained state for a period of 20 minutes.

These curves essentially superimpose on one another on stretching showing that the repeatability of the experiments is quite good. The rate of stress relaxation increases with total stretching levels imposed on the films. The family of curves obtained for lower crosslink density samples all show lower stress levels for given extension resulting for lower crosslink density.

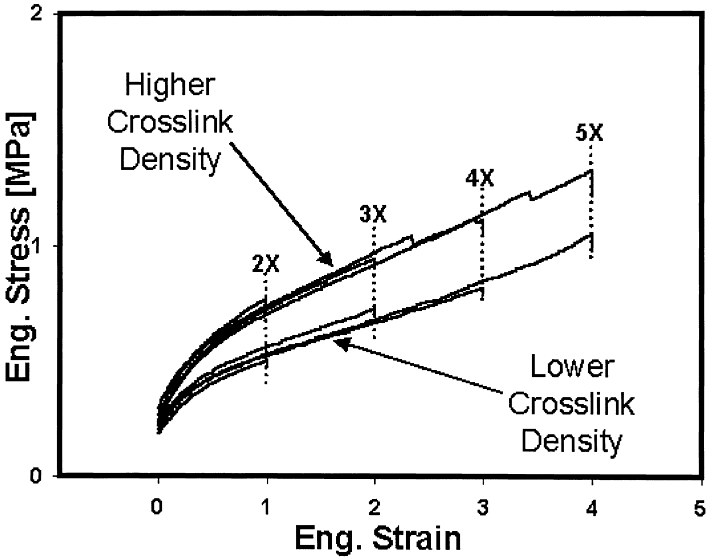

Figure 2. Mechanical response of NR. Engineering stress vs. engineering strain.

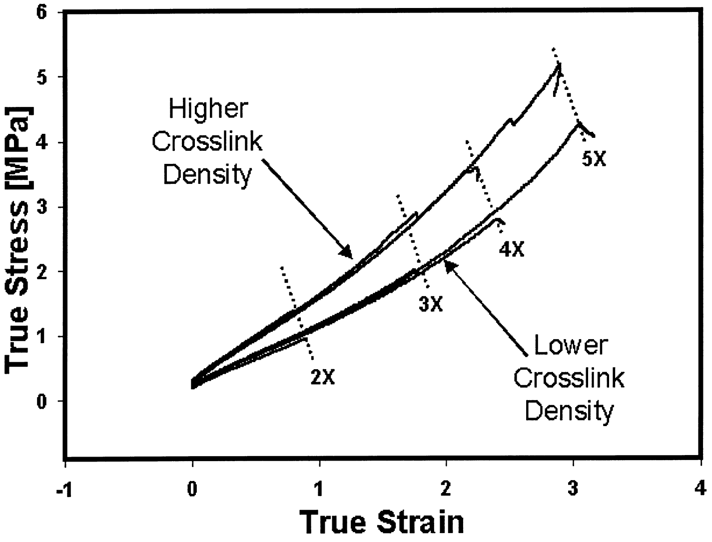

Figure 3. Mechanical response of NR. True stress vs. true strain.

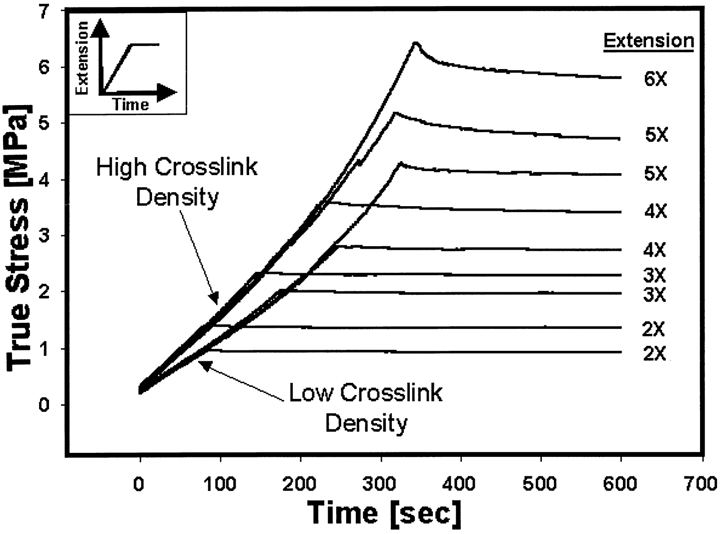

Figure 4. Mechanical response of natural rubber. True stress vs. time.

Birefringence Measurements

Figure 5 and Figure 6 shows the behavior of birefringence vs. true strain and birefringence vs. time respectively for the high crosslink density material stretched to different levels and held for 20 minutes. An increase of birefringence is observed for both cases occurring from the beginning of the stretching. Off-line measurements of birefringence vs. strain done in the past[15] indicate small increases of birefringence at low extensions and a sudden steep increase at high levels of stretching. Our real-time birefringence system allows us to monitor the molecular reorganization during stretching in a more realistic manner showing an increase of birefringence much closer to the linearity through out the whole stretching process. However, a slight increase of slope can still be observed at larger levels of extension.

The birefringence behavior with time for different crosslink densities is shown in Figure 7. The WAXS patterns taken at the end of the relaxation (constrained period) are also included in order to monitor the crystallinity development during the stretching. The values of birefringence are always higher for the high crosslink density material. The crystallinity as shown by the WAXS patterns clearly develops earlier for the lower crosslink density. The curves stretched to higher levels (compare 5x in Figure 7) reveal more intense reflections from different crystallographic planes in the case of the lower crosslink density material than that observed for its higher crosslink counterpart. This is due to the build up of certain level of molecular orientation required for the crystalline domains to form. The increase of junction points between the chains through chemical bonds inhibits the molecular motion, which in turn decreases the ability to orient along the direction of the deformation for further crystallization.

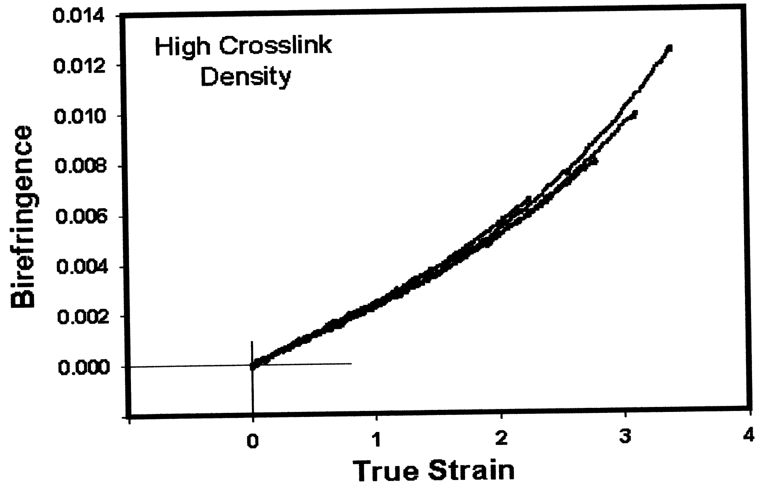

Figure 5. Birefringence vs. true strain for the high crosslink density material stretched tc several extends.

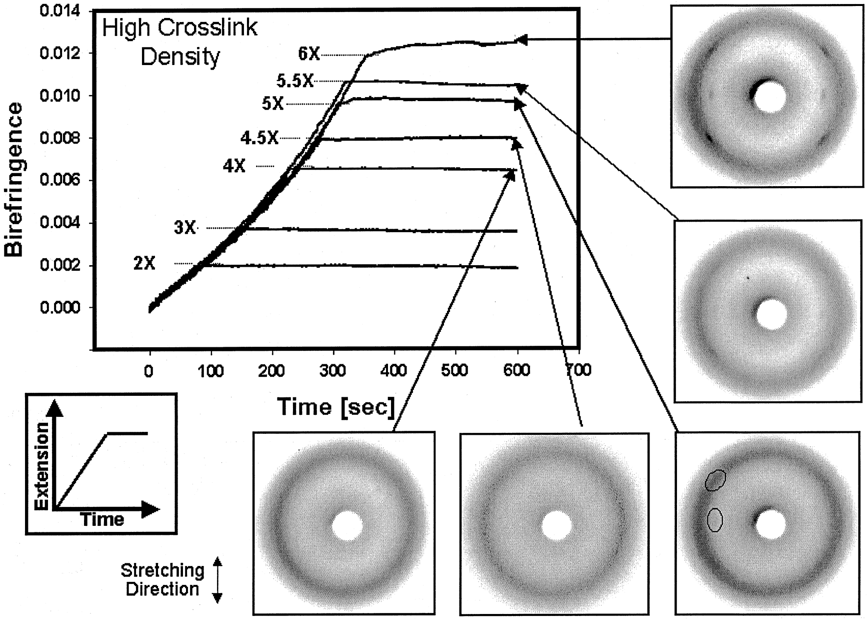

Figure 6. Birefringence vs. time for the high crosslink density material stretched to several extends.

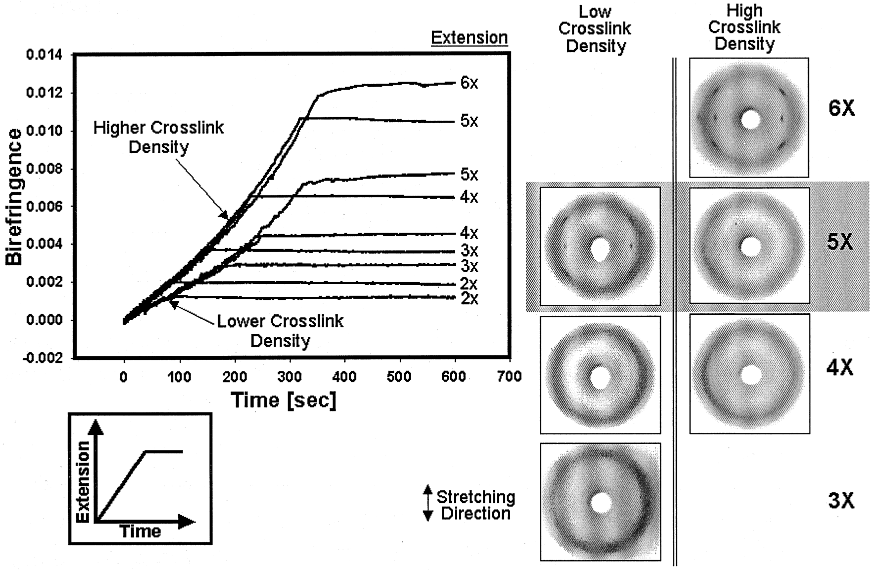

Figure 7. Birefringence vs. time for the two crosslink densities stretched to several extends.

Relaxation Mechanism

The investigation of molecular behavior immediately after stretching when the samples were still in constrained state was important to understand the mechanisms behind the relaxation process. For this purpose, we built a curve that conveys the starting point of the relaxation (for each extension) to the same zero-birefringence value. This curve is presented in figure 8; which also includes the X-ray patterns for highly stretched samples.

All of the samples stretched to low deformation levels show similar relaxation behaviors in that the birefringence does not vary from the original value recorded immediately after stretching. However, highly stretched samples (6x) clearly deviate from this constant behavior exhibiting a big jump in birefringence values during the relaxation. This is attributed to the crystallization of the rubber during the relaxation phase. This increase is temporary at lower deformation levels (5x) and begins to decrease at long times suggesting that the relaxation of oriented but amorphous chains dominates the birefringence development. However at higher deformation levels this decrease is not observed instead a gradual approach to plateau behavior is observed.

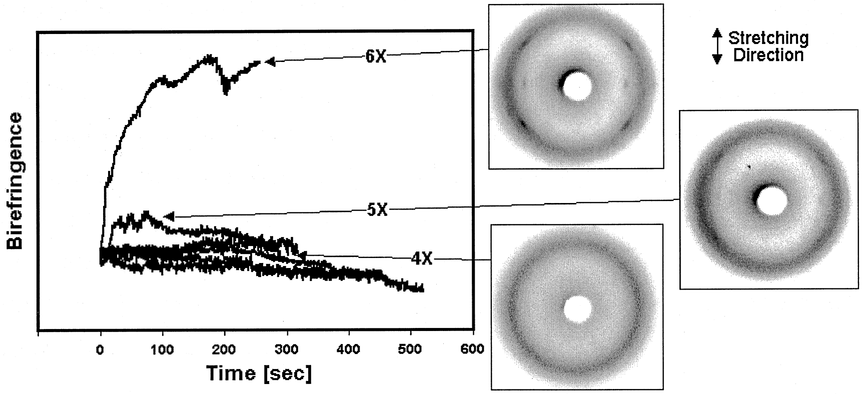

Figure 8. Relaxation of the birefringence for the high crosslink density material stretched to several extends.

Stress-Optical Law Analysis

The stress optical law relates the birefringence and stresses applied in a system. The law follows a linear behavior of the birefringence with the stress for amorphous polymers expressed as shown in equation 2:

$$\Delta n = C \cdot \sigma \qquad \text{Eq. 2}$$

Where:

Δn = Birefringence

C = Stress-optical Coefficient

σ = Stress

The calculation of the stress-optical coefficient has been a difficult task through conventional off-line methods due to tedious and time-consuming work needed to carry out the optical measurements during the deformation. This new spectral-birefringence technique allows very quick and precise determination of the stress optical law by simultaneous measurements of real time birefringence and true stress.

Figure 9 shows the stress optical law behavior for natural rubber samples of two different crosslink densities stretched to several extents. The graph was built from the data obtained during stretching of the samples. All the curves lay down on the same straight line regardless of the crosslink density or the degree of deformation of the rubber. Even for high extension ratios when crystalline domains are present (as observed from the WAXS patterns), the behavior does not deviate from the linearity. Using equation 2 the stress optical coefficient was determined to have a value of $C=1.8GPa^{-1}$ that is in good agreement with values reported in earlier studies.[16]

A peculiar behavior is the continuous linearity experienced for samples stretched to high levels of extension where indications of strain-induced crystallization are observed. In order to study this phenomenon and have a better understanding of what is happening during the deformation, we modified Figure 9 including the data obtained during the relaxation of the rubber as well as the WAXS patterns for each extension. The results are shown in Figure 10. It is clear to observe the formation of "tips" at the end of each stretching that progressively increase in length at higher stretch ratios. These "tips" are coming from the data recorded during the relaxation period and they appear when crystalline domains are observed in the X-ray patterns. As a result, the deviation from the linearity of the stress-optical law indicates that the crystallization is taking place during the relaxation of the rubber. This is in good agreement with previously discussed Figure 8 where a big jump in the birefringence takes place during the relaxation right when the crystallization is observed.

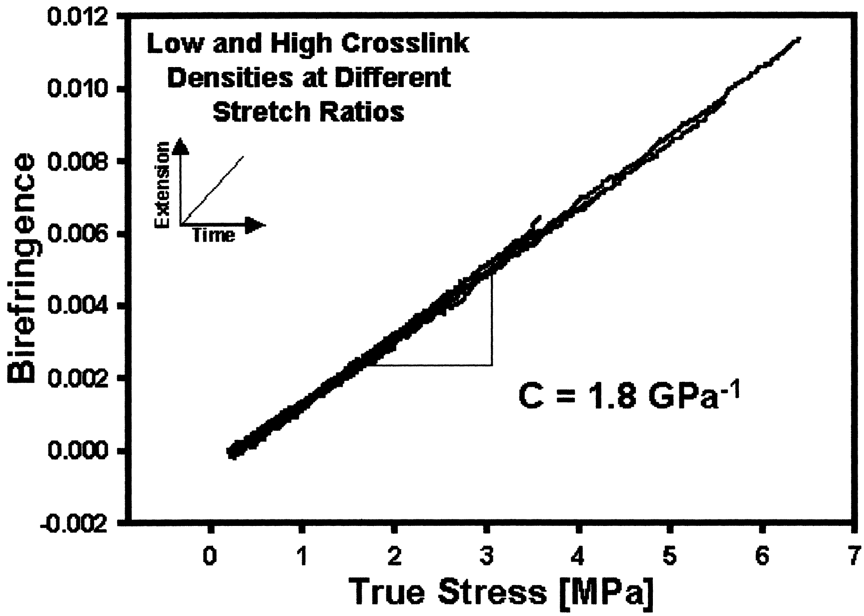

Figure 9. Stress-Optical Law. Data obtained during the stretching of natural rubber samples of different crosslink densities at several extensions.

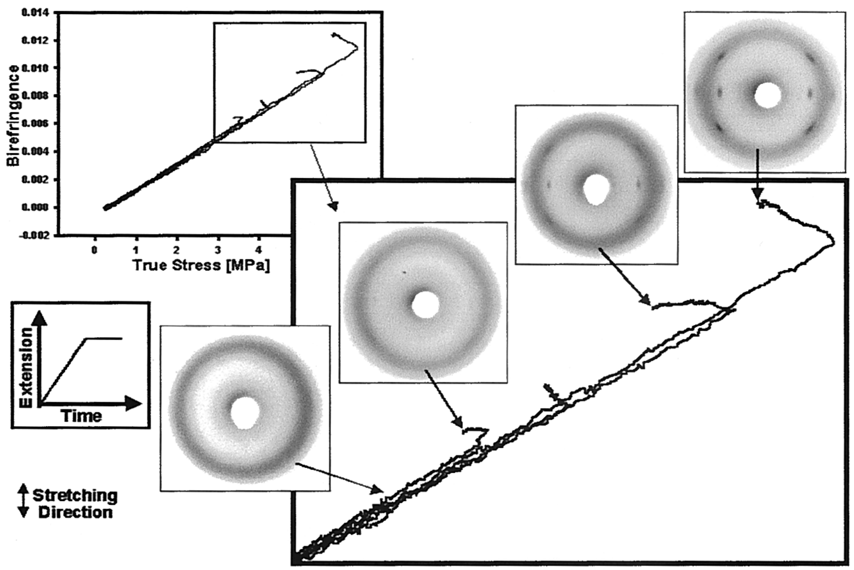

Figure 10. Stress-Optical Law. Data obtained during the stretching+relaxation of natural rubber samples of different crosslink densities at several extensions.

Hysteresis Analysis

Hysteresis is the phenomenon seen in elastic and electromagnetic materials in which a lag occurs between the application and removal of a force or field. Natural rubber shows hysteresis of the true stress vs. true strain. The behavior of samples stretched to 2x, 3x, 4x and 5x at room temperature and subsequently retracted to zero is shown for the high crosslink density material in Figure 11.

The hysteresis loop increases as the sample is stretched to higher ratios. This is a consequence of different mechanisms of deformation during stretching and retraction. During the stretching of the complex original network, composed of chemical (sulfur bonds) and physical (entanglements) crosslinks, the molecules re-organize as a result of the applied deformation. When the deformation is high enough, some of the chemical bonds will break and part of the physical network will disentangle. The sulfur-sulfur bonds will preferably break over the carbon-carbon bonds since they have lower dissociation energy (64 kcal/mole vs. 83 kcal/mole).[17] Further in the deformation, the crystalline domains begin to form and may link different molecules making the network even more complex. However, the broken chemical crosslinks will not re-form during the retraction of the sample; as well as the entanglements will not develop at the same original positions. These variations lead to an energetic difference that is reflected in the hysteresis curve by the formation of the loop. For instance, there is no evidence of hysteresis at very low deformations (2x) since at this point the network has not suffered any irreversible changes.

Figure 12 shows the comparison of hysteresis for two crosslink density samples stretched 5 times their original size. Higher stresses are always experienced for the high crosslink density material. The area enclosed in the hysteresis loop of these curves clearly increases for the high crosslink density. This is again a consequence of the molecular deformation mechanism during stretching and retraction of the rubber samples. The higher amounts of sulfur-sulfur bonds in the high crosslink density material interact with the rearranging molecules leading to the breakage of the chemical network. For that reason, the high crosslink density samples experience more irreversible energetic changes that are going to be reflected in the hysteresis curve by an increase of the loop area.

Birefringence also shows hysteresis with true stress. The results are observed in Figure 13 for a high crosslink density sample stretched 6 times its original length. For the birefringence-true stress analysis, the WAXS patterns were included at several positions during the extension as well as during retraction of the samples. This curve is of great importance because it indicates when the crystalline domains appear during the extension and disappear during the retraction. These values of birefringence are very close to each other even though the trajectories of the birefringence are very different during each deformation process. Therefore, it appears to exist a critical value of birefringence above which the crystallinity takes place and this value is around $\Delta n=0.008$ for the high crosslink density rubber considered in this study.

Figure 14 shows the behavior of birefringence vs. true strain during extension and retraction for both crosslink density samples stretched to 5x. The results indicate that there is no hysteresis of the birefringence with the true strain. This peculiar behavior has not been observed before and it is attributed to the nature of the true strain data. The values of true strain are determined by the continues data acquisition of sample width through the laser micrometer mounted in the stretching device, which allows us to determine the dimensions of the samples at all times during the deformation. Therefore, the true strain data already includes the dimensional changes produced both by the morphological changes (crystallinity) and deformation.

In the previous discussion where there is a clear indication of the true stress-true strain hysteresis, the true strain also includes the dimensional changes monitored during the whole deformation process. However, the true stress takes into account the force data recorded by the load cell at all times. As discussed before, there are energy levels to achieve during the extension in order to break the chemical bonds linking the molecules, which are not required during the retraction since there is no sulfur-sulfur bond reformation. As a result, the true stress shows hysteresis with the true strain.

In order to support the previous discussions, Figure 15 shows the behavior of birefringence with engineering strain for the same high crosslink density sample stretched 5 times its original length. In this case, the engineering strain only considers the original dimensions of the sample and the presence of the hysteresis loop can be clearly distinguished.

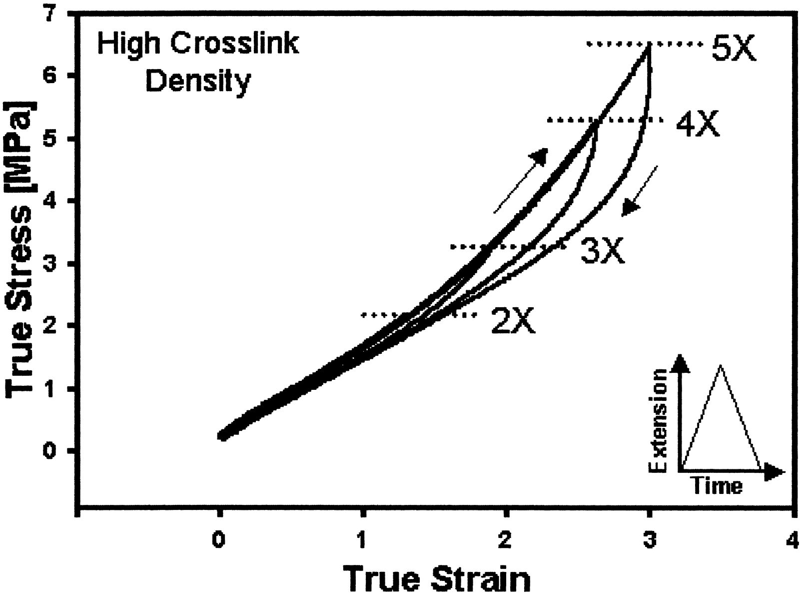

Figure 11. True stress-true strain hysteresis behavior. High crosslink density material stretched to 2x, 3x, 4x and 5x at room temperature and then retracted to zero.

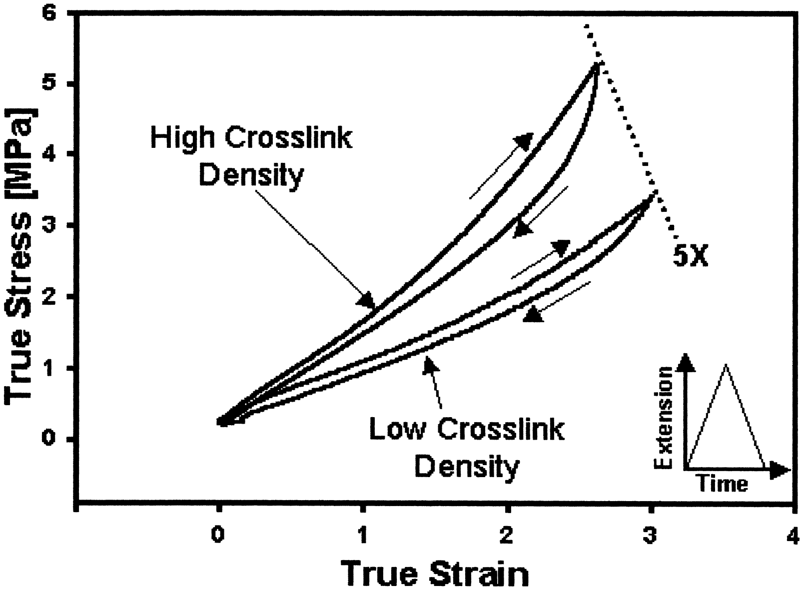

Figure 12. True stress-true strain hysteresis behavior. Low and High crosslink density material stretched to 5x at room temperature and then retracted to zero.

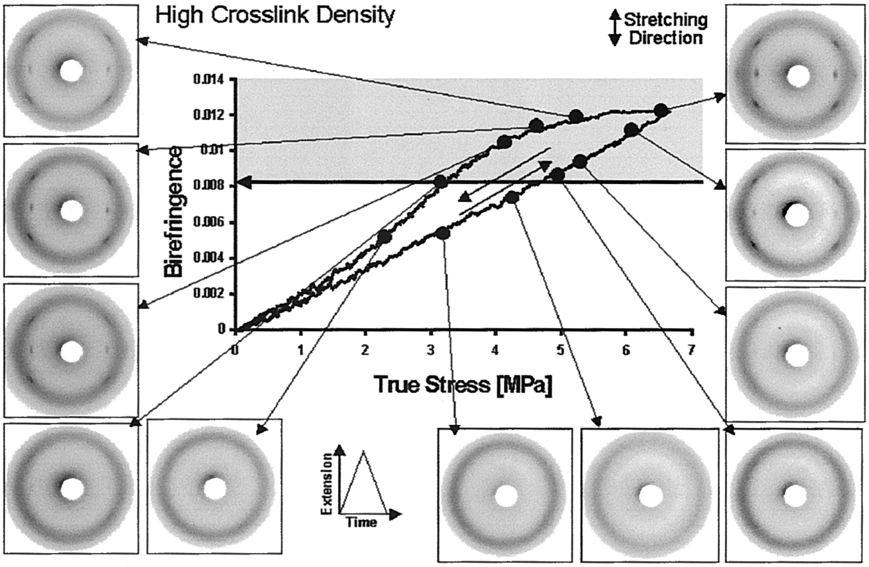

Figure 13. Birefringence-true stress hysteresis behavior. High crosslink density material stretched to 6x at room temperature and then retracted to zero.

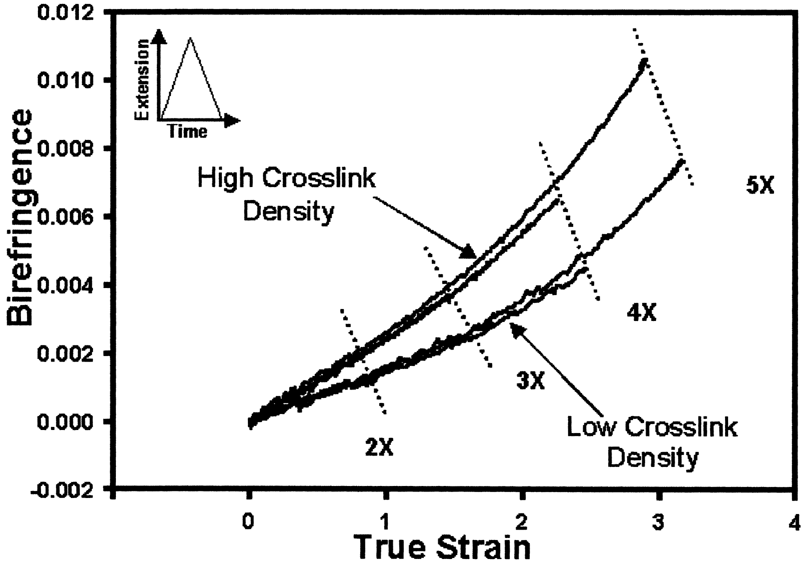

Figure 14. Birefringence-true strain hysteresis behavior. Low and High crosslink density material stretched to 2x, 3x, 4x and 5x at room temperature and then retracted to zero.

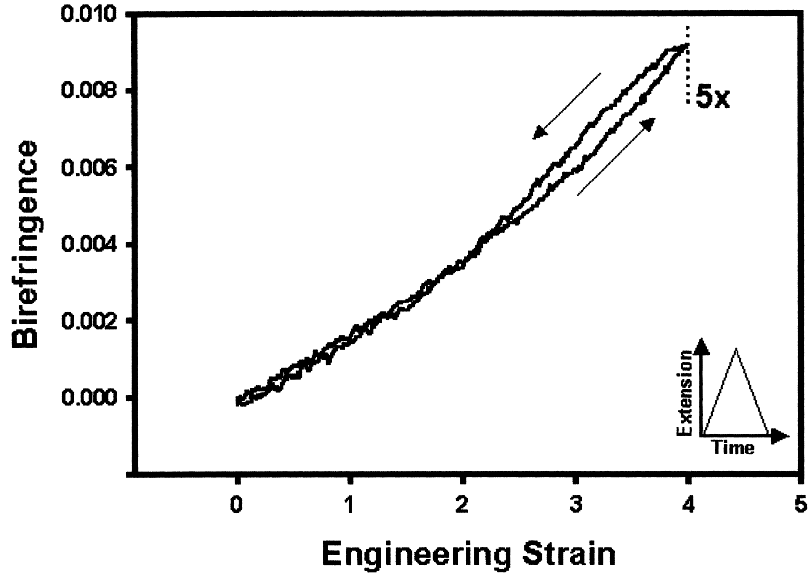

Figure 15. Birefringence-engineering strain hysteresis behavior. High crosslink density material stretched to 5x at room temperature and then retracted to zero.

Model

As described in great length above, the structural formation mechanism in crosslinked natural rubbers can be described in Figure 16; where schematically the structural ordering processes are depicted. At room temperature the natural rubber is above its effective melting temperature and behave as if it is a melt. The only structural features to observe are the crosslinks that were formed chemically during the curing and the physical network composed by the molecular entanglements. In our investigations we varied the crosslink density to illustrate its effect. The real time measurements indicate that the early stages of deformation occur by progressive orientation of polymer chains along the stretching direction as dictated by the level of true stresses applied. In this stage the material does not exhibit hysteresis if retraction is applied. Further stretching leads to the distortion of the network by breakage of chemical bonds and disentangle of the molecules. After this point of deformation, hysteresis is noticeable during retraction due to irreversible changes occurred in the rubber network. As the stretching proceeds, "near perfectly" oriented chain segments are formed. The results indicate that if the deformation stops and the material is kept held, these highly oriented chains are able to pack together for the formation of crystalline domains. We suspect these regions are in the close proximity of the chemical crosslinks as well as the physical networks that transmit externally applied forces to their vicinity most efficiently. The presence of extremely narrow azimuthal intensity distribution of the equatorial crystalline peak representing the interchain correlation and absence of off-equatorial crystalline peaks describes a structure where the crystalline regions that are occupying a small fraction of the volume ~10-20% are composed of very highly oriented chains aligned with poor axial registry with each other. The results also suggest that the further stretching brings about crystallinity of the regions with lesser preferential orientation resulting in increased azimuthal spread of the interchain correlation peak.

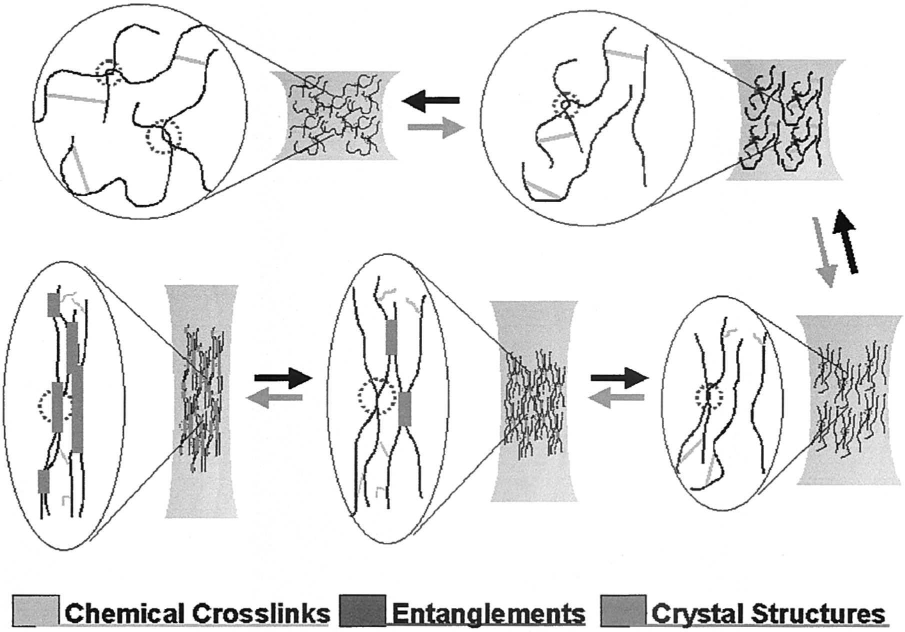

Figure 16. Molecular deformation of Natural Rubber vulcanizates during uniaxial extension.

Conclusions

We have successfully developed a robust stretching/spectral birefringence device, which allows us to measure true stress, true strain and real time birefringence simultaneously at 0.4 second intervals during stretching. This technique was found to be sensitive enough to follow the small changes in retardation in the natural rubber that inherently possesses low intrinsic birefringence.

The results on crosslinked rubbers indicate a continuous molecular orientation taking place during the stretching. At high enough extension ratios, the crystallization takes place during the relaxation (or constrained stretched state) of the rubber. The chemical crosslink greatly affects the crystallization as they inhibit the molecular reorganization. Higher crosslink density natural rubber achieves higher stresses and lower crystallinity levels at the same stretch ratios.

This technique allowed very quick and precise determination of the stress-optical coefficient. This birefringence-true stress relationship indicates that the crystallization of rubber takes place during the relaxation process. It also shows hysteresis between stretching and retraction. The hysteresis behavior and the WAXS patterns allowed us to determinate a critical value of birefringence above which the crystallinity takes place.

[1] H. H. Yang, M. P. Chouinard and W. J. Lingg, *J. Polym. Sci. Polym. Phys.*, **1982**, *20*, 981

[2] G. F. Harding. "*Optical Properties of Polymers*". G. H. Meeten. 1986

[3] M. Pluta, *Polymer*, **1992**, *33*, 1553

[4] K. Hongladarom, W. R. Burghardt, S. G. Baek, S. Cementwala and J. J. Magda. *Macromolecules*, **1993**, *26*, 772

[5] K. Hongladarom and W. R. Burghardt, *Macromolecules*, **1993**, 26, 785

[6] K. Hongladarom, V. Secakusuma and W. R. Burghardt, *J. Rheol.*, **1994**, *38*, 1505

[7] W. R. Burghardt and K. Hongladarom, *Macromolecules*, **1994**, *27*, 2327

[8] F. Beekmans and A. Posthuma de Boer, *Macromolecules*, **1996**, *29*, 8726

[9] T. F. Serhatkulu and M. Cakmak. *SPE ANTEC Tech. Pap.* **1999**, 1645

[10] G.Kokturk, T.F.Serhatkulu, A.Kozluca, E.Piskin, M.Cakmak. *SPE ANTEC Tech. Pap.* **1999**, 2190

[11] G Kokturk, T.F Serhatkulu, and M. Cakmak. *SPE ANTEC. Tech. Pap.*, **2000**, 1737

[12] S. Toki, D. Valladares, T. Z. Sen and M. Cakmak. *SPE ANTEC Tech. Pap.*, **2001**, 1830

[13] Y. H. Zang, R. Muller, D. Froelich, *Polymer*, **1989**, *30*, 2060

[14] H. Oikawa, K. Murakami, *Rubber Chem. Tech.*,**1987**, *60*, 579

[15] C. M. Roland. *Macromolecules*, **1996**, *29*, 6941

[16] P. H. Mott and C. M. Roland. *Macromolecules*, **2000**, *33*, 4132

[17] J. A. Brydson "*Plastic Materials*". Butterworths, 5th Edition. London. 1989